Stress wave propagation in a centrifuge model

S.P.Gopal Madabhushi

CUED/D-SOILS/TR272 (1994)

SYNOPSIS

Shear modulus of a soil layer increases with the effective confining stress. This results in a reduction in the propagation velocity of shear waves as they travel from the bed rock towards the soil surface. In a centrifuge model prototype stresses and strains are recreated at homologous points. Thus the effective confining stress and hence the shear modulus will vary with depth in a centrifuge model. This results in a change in the propagation velocity of the shear waves as they travel from the base of the container towards the soil surface. This change in the propagation velocity was investigated by performing non-linear finite element analyses using simple single pulse and sinusoidal ground motion. as well as more realistic bed rock accelerations. Based on the results from these analyses it was concluded that the variation of shear modulus with effective confining stress results in a reduction in the propagation velocity as the shear waves travel to soil surface. Also the frequency of the input bed rock motion suffers some dispersion.

The delay in the arrival of shear waves at the surface of the centrifuge model results in a phase difference between the acceleration recorded at the base of the model container and acceleration recorded at the soil surface. This will be especially so when the centrifuge model consists of a deep soil bed. The results from the present analyses will be important as there will be a need to distinguish from the phase difference arising from the delay mentioned above and the phase difference which indicates if the soil is under resonant conditions.

INTRODUCTION

During a seismic event stress waves are induced in the bed rock following a slip along the fault plane. These stress waves travel over long distances within the bed rock. They are also propagated through the overlying soil towards the surface of the soil bed as shown in Fig. 1. If we wish to model the seismic behaviour of a civil engineering structure founded in such a soil bed we must understand the propagation of stress waves through the soil. During the Mexico city earthquake of 1983 and more recently in the Northridge earthquake of Los Angeles in 1994 it was observed that the soil properties greatly contribute to the amplification or attenuation of stress waves as they travel through the soil bed. This can be readily observed by plotting the distribution of damage in the districts surrounding the epicentre. For example, during the Northridge earthquake of' Los Angeles the Marina Del Ray district closer to the epicentre and adjacent to severely damaged Santa Monica district suffered little damage compared with the King Harbour area on Redando beach which is much farther away from the epicentre, Madabhushi (1994).

In this paper an effort will be made in understanding the propagation of stress waves through a horizontal sand bed For brevity only vertically propagating horizontal shear (S_h) waves will be considered. It has been established that the shear modulus of a soil layer varies with the confining stress. Hardin and Dmevich (1972) have suggested that the variation of shear modulus with the effective confining stress is non-linear and can be approximated for most soils as a square root function. The non-linear variation in shear modulus will result in. a change in the propagation velocity of the shear waves

within the soil layer and contribute to the change of frequency of the bed rock motion as it travels towards the soil surface. These effects will be investigated in this paper.

DYNAMIC CENTRIFUGE MODELLING

Dynamic centrifuge modelling has evolved as a powerful technique to study the seismic response of soil-structure interaction systems. This technique involves subjecting reduced scale models placed in the increased gravitational environment of a geotechnical centrifuge to model earthquakes. The dynamic behaviour of the model is related to the prototype behaviour by a set of scaling laws, Schofield (1980,81), as shown in Table 1. From the table it can be seen that the prototype stresses and strains are recreated in the centrifuge model at the homologous points. In fact, this is the principle advantage of centrifuge modelling as the stress-strain behaviour of the soil is accurately modelled by this technique.

Let us now consider a centrifuge model with a horizontal layer of sand as shown in Fig.2. In a geotechnical centrifuge this model is subjected to a centrifugal acceleration of 'ng'. The equivalent prototype this centrifuge model would represent will have a width of 'nb' and a height of 'nh'. The model container is subjected to lateral shaking to simulate the earthquake loading. At Cambridge University this is done by means of a mechanical excitation system called the 'Bumpy Road' actuator. The principle and working of this system is discussed by Kutter, (1982). As a result of this vertically propagating horizontal shear waves are produced in the soil layer. The end walls of the model container are designed to have approximately the same dynamic stiffness as

the equivalent shear column of soil so that no end reflections will result during the lateral shaking.

WAVE PROPAGATION IN CENTRIFUGE MODELS

From the scaling laws for stresses and strains (see Table 1) we have seen that the prototype stresses and strains are recreated at homologous points within the centrifuge model. In the centrifuge model with horizontal sand layer the effective confining stress increases with the depth similar to the prototype sand bed it represents. This would mean that the shear modulus of the soil layer in the centrifuge model would increase with the increase of the effective confining stress or in other words with the depth of the soil layer. This will in turn result in a variation of propagation velocity of shear waves with the depth of the centrifuge model.

Let us focus on the vertically propagating horizontal shear (S_h) waves within the centrifuge model. The lateral shaking of the model container induces horizontal shear waves at the base of the model akin to the bed rock motion. As the shear waves travel upwards towards the surface of the soil they will encounter soil elements with less and less shear stiffness as the effective mean confining pressure reduces towards the soil surface. This would mean that there will be a reduction in the propagation velocity of the shear waves (S_h) as we move from the base of the container towards the soil surface. Also there will be a change in the frequency of base motion as it propagates towards the surface.

SEMI-INFINITE HORIZONTAL SAND BED

The change in propagation velocity will induce a time delay effect as the waves travel to the soil surface. An understanding of this is important especially when phase relationship between acceleration records at different depth is used to determine if the soil layer is under resonance, for example Steedman and Zeng (1993). The change in propagation velocity is difficult to determine directly from the centrifuge experiments due to the extremely small time scales involved in these tests. However it is possible to investigate the variation of the propagation velocity of shear waves in a horizontal sand bed by performing non-linear finite element analyses in the time domain. For the purpose of these analyses a 1.5m horizontal sand bed overlying on the bed rock (as in Fig.l) is chosen as the bench mark problem. The propagation of shear waves (St,) in such a sand bed can be studied by considering a column of soil as shown in Fig.3. The nodes on either side of the soil column are restricted in the vertical direction but are free to move in the horizontal. direction to facilitate the propagation of the S_h waves. The shear modulus of the soil increases with the depth of the soil layer as explained in the next section.

Two types of FE analyses were performed. In the first type of analysis a single pulse of shear wave (S_h) was used as the input motion at the base nodes. The propagation of this pulse at different heights is monitored to determine the change in the shear wave velocity. Also the change in the frequency of input motion is observed. In the second set of analyses more realistic earthquake input motions are applied at the base nodes.

NON-LINEAR FINITE ELEMENT ANALYSIS

The shear wave (S_h) propagation in the soil column shown in Fig.3 was investigated by using a finite element program called SWANDYNE, Chan (1988). SWANDYNE is an effective stress program which uses unconditionally stable Wilson-0 formulation for time marching. The time steps for the wave propagation problem, however, must be chosen based on the velocity of propagation and the frequency of the input motion. The resulting wave length must be a fraction of the grid dimensions. In this program it is possible to vary the shear modulus of the soil layer with depth using the following equation;

$$G = G_o \left[p_o / p_{ref} \right]^{\alpha} \qquad ...(1)$$

where G is the shear modulus at any depth where the mean effective confining stress is p_o, G_o is the reference shear modulus measured at a depth where the mean effective confining stress is p_{ref}. In all the analyses the value of G_o was 43 MPa. Also the soil density and void ratio were 1472.2 kg/m^3 and 0.8 respectively. This gives the reference shear wave velocity of 170.9 m/s. The constitutive model used in the present analysis was a non-linear elastic model described by Chan, (1989).

F.E. ANALYSES WITH SIMPLE INPUT MOTION

The finite element mesh used for these analyses consisted of 600 four noded quadrilateral elements. The element size in the direction of S_h wave propagation was chosen such that it is only a fraction of the wavelength of the shear wave. The bed rock motion was applied as a time varying displacement during these analyses. The wave propagation was monitored at different depths in the soil column by plotting the displacement at nodes listed in Table 2. A nominal damping of 5% is used in all the analyses as only dry sand was modelled.

Single Pulse Input Motion

In Fig.4 the results of a single pulse S_h wave propagating in the soil column when there is no variation in the shear modulus with depth (Case 1 in Table 3) are presented. The shear pulse is applied at the base nodes (see Node 4 in Fig.4). The propagation of this wave towards the surface can be observed by noticing the arrival times at nodes 3,2 and 1 which are 0.03s, 0.059s and 0.089s respectively. These arrival times confirm the shear wave velocity is indeed 170.9 m/s. The shear wave pulse is then reflected from the free surface and travels towards the bed rock and in turn is reflected back. Several reflections can be observed before the end of the analysis. In Fig.5 the results of an identical S_h wave pulse propagation in a soil column whose shear modulus varies with depth (Case 2 in Table 3) are presented. By comparing this figure with Fj.g.4 the delay in the arrival of shear wave at nodes 3,2 and 1 can be clearly seen. The arrival times of the S_h wave pulse at these nodes are 0.055s, 0.105s and 0.163s which show that the shear wave is progressively slowed

down as it travels towards the surface. During the analysis the shear wave velocity at many more nodes were obtained and the velocity profile with depth is plotted in Fig.7. The results from the analysis performed using Case 3 parameters (see Table 3) is presented in Fig.6. By comparing this figure with Figs.4&5 it can be seen that the shear wave propagation is further delayed when the exponent of shear modulus variation (a) is increased to 0.25. The arrival times at nodes 3,2 and 1 in this case were 0.12s, 0.241s and 0.372s showing progressive delay as the wave travels to the soil surface. The velocity profile with depth for this analysis is also presented in Fig.7.

Continuous Sinusoidal Input Motion

In the second set of analysis a continuous single frequency (100 Hz) sinusoidal displacement is applied at the base nodes. The dispersion in the frequency of the bed rock motion as it travels through the soil layer was investigated. In Fig.8 the results from the analysis performed using Case 1 parameters (see Table 3) are presented. As there is no variation in shear modulus the S_h wave train travels towards the soil surface rapidly. Reflections from the free surface result in the change in amplitude as observed at nodes 4,3 and 2. As node 1 is very close to the free surface the sinusoidal motion is almost nullified after the first half cycle. However the frequency of the S_h wave train does not change at any node. In Fig.9 the results from a similar analysis but using Case 3 parameters is presented. On the left hand side of this figure the progressively delayed S_h wave is presented. On the right hand side the frequency analyses of the corresponding, displacement time histories are presented. In this figure it can be seen that there is a gradual dispersion in the frequency response about the 100 Hz mark as the S_h wave travels towards the surface. A further analysis was

carried out in which the exponent of the shear modulus variation (a in Eq.l) was 0.5. The frequency analyses at the corresponding four nodes are presented in Fig.10. The dispersion in the frequency as the wave travels towards the soil surface is more pronounced in this analysis.

Based on the above analyses with single pulse and continuous sinusoidal wave inputs it may be concluded that the variation of shear modulus with depth results in a progressively slowing down cd the S_h waves and causes a dispersion in the frequency of bed rock motion as the shear waves travel towards the soil surface.

F.E. ANALYSES WITH REALISTIC BED ROCK MOTION

In this series of analyses realistic ground accelerations were applied to the base nodes of the soil column in Fig.3. Also S_h wave propagation is monitored by plotting the accelerations as opposed to the displacements plotted in the previous analyses. Two types of bed rock accelerations will be considered. First the ground motion generated by the 'Bumpy Road' actuator (Kutter, 1982) at the Cambridge University was used. This actuator produces approximately 10 cycles of single frequency base shaking which lasts for about 0.1s. In a '8Og' centrifuge test the fundamental frequency of the base motion is 120 Hz (1.5Hz in the prototype earthquake). The acceleration tune history from a typical centrifuge test was applied to the base nodes of the soil column. In Fig.1 1 the results of the analyses performed using Case 1 parameters (no shear modulus variation) are presented. In this figure the propagation of the base acceleration through different: nodes can be clearly seen. Also the reflection from soil surface can be observed at nodes 2 and 3. In Fig.12 the results from a similar analysis

using Case 3 soil properties is presented. Notice that the duration of this analysis was twice of that shown in Fig.1 1. On the left hand side of Fig. 12 the acceleration time histories are presented and on the right hand side corresponding frequency analyses are presented. Comparing Figs.1 1&12 we see that the variation in shear modulus has resulted in progressive slowing of the propagation of base acceleration towards the soil surface. Also there is significant difference in the frequency analyses at different nodes.

A second analysis was carried out using the ground accelerations recorded at the toe of the Pyramid Dam near Los Angeles during the 1994 Northridge earthquake. The time base of this acceleration history was scaled using the centrifuge scaling laws (see Table 1) for a '80g' centrifuge test. This modified acceleration history was applied to the base nodes of the soil column. In Fig.13 the results from the analysis performed using Case 1 parameters (see Table 3) are presented. The acceleration time history is propagated through the soil as seen at different nodes in this figure. Also the free surface reflections result in longer accelerations at nodes 2 and 3. In Fig.14 the results from the analysis performed using Case 3 parameters (see Table 3) are presented. On the left hand side the accelerations at different nodes are shown. Corresponding frequency analyses are presented on the right hand side. Comparing Figs. 13&14 the progressive slowing of the shear waves as they travel towards the soil surface is noticed. The frequency analysis of the time histories at various nodes is significantly different. Also the higher frequencies above 500 Hz (6.25 Hz in the prototype earthquake) are not propagated through the soil layer. This may be due to the limiting dimension of the FE mesh itself.

CONCLUSIONS

Shear modulus of a soil layer varies with the effective confining stress. This results in a reduction in the propagation velocity of a shear wave travelling from the bed rock towards the soil surface. This effect will also be present in a dynamic centrifuge test as the confining stresses in the centrifuge model truly represent those in a prototype soil layer. The variation in the propagation velocities of shear waves in a soil layer were investigated by conducting non-linear FE analyses. Using single pulse and continuous sinusoidal input motions the delay in the propagation of the shear waves in a soil layer as they travel towards the surface and frequency dispersion of the input motion were established. These effects were also observed when more realistic earthquake motions were applied to the bed rock. These results will be significant when interpreting the dynamic centrifuge test data consisting of deep soil layers as the change in shear wave velocity with depth will cause a time delay effect resulting in the phase shift between the accelerations recorded at the base and at the surface of the soil.

REFERENCES

Chan, A.H.C.,(1988), A unified finite element solution to static and dynamic problems in Geomechnanics, Ph.d thesis, University College of Swansea, Swansea.

Chan, A.H.C.,(1989), User manual for Diana-Swandyne-II, Department of Civil Engineering, Glasgow University, Glasgow.

Kutter, B.L., (1982), Centrifugal modelling of response of clay embankments to earthquakes, Ph.d thesis, Cambridge University, England.

Hardin, B.O. and Drnevich,V.P.,(1972), Shear modulus and damping in soils: Design equations and curves, Proc.ASCE, JSMF Div., No.98., SM7.

Madabhushi, S.P.G., (1994), Geotechnical Aspects of the Northridge Earthquake of 17 January, 1994 in Los Angeles, EEFIT Report, Institute of Civil Eng., UK.

Schofield, A.N.,(1980), Cambridge geotechnical centrifuge operations, Geotechnique, Vol.25., No.4, pp 743-761.

Schofield, A.N.,(1981), Dynamic and Earthquake geotechnical centrifuge modelling, Proc. Recent Advances in Cieotech. Earthquake Eng. Soil dynamics and earthquake eng., Univ. of Missouri-Rolla, Rolla.

Steedman, R.S. and Zeng,X.,(1993), Modelling of seismic behaviour of quay walls, Geotechnique, Vo1.42.

Table 1 Scaling laws

Parameter	Ratio of model to prototype
Length	1/n
Area	$1/n^2$
Volume	$1/n^3$
stress	1
Strain	1
Force	$1/n^2$
Velocity	1
Acceleration	n
frequency	n
time (dynamic)	1/n
time (consolidation)	$1/n^2$

Table 2 Depth of nodes below soil surface

Number	Depth below soil surface (m)
Node 1	0.01
Node 2	5.0
Node 3	10.0
Node 4	15.0

Table 3 Soil Properties in different analyses

Parameter	Case 1	Case 2	Case 3
Reference Shear Modulus (G_r)	43 MPa	43 MPa	43 MPa
Soil Density	1472.2 kg/m^3	1472.2 kg/m^3	1472.2 kg/m^3
void ratio (e)	0.8	0.8	0.8
Shear Modulus variation	constant	varying	varying
Reference confining stress (p_{ref})	--	30 kPa	30 kPa
Exponent of variation (α)	--	0.1	0.25

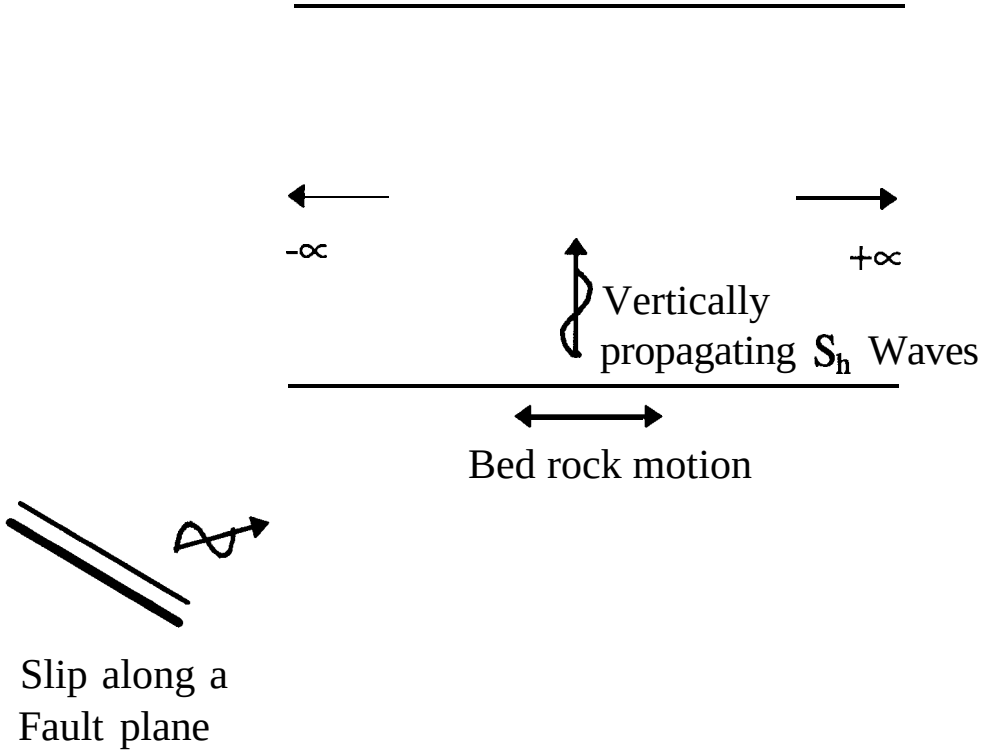

Fig. 1 Propagation of stress waves

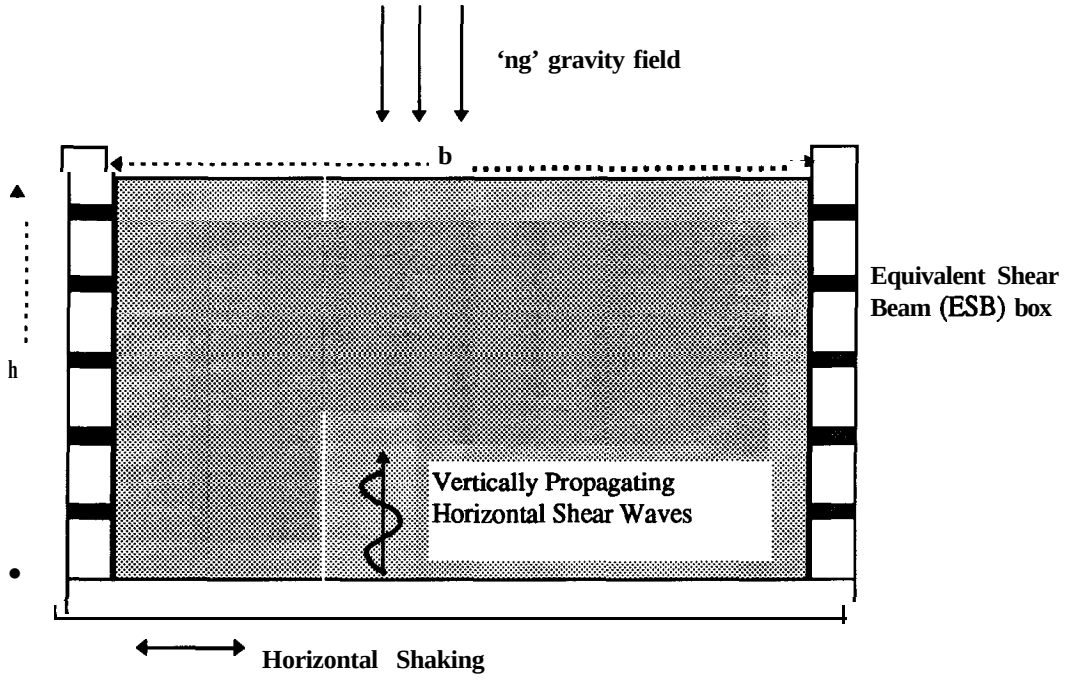

Fig.2 Centrifuge Model of a horizontal sand bed

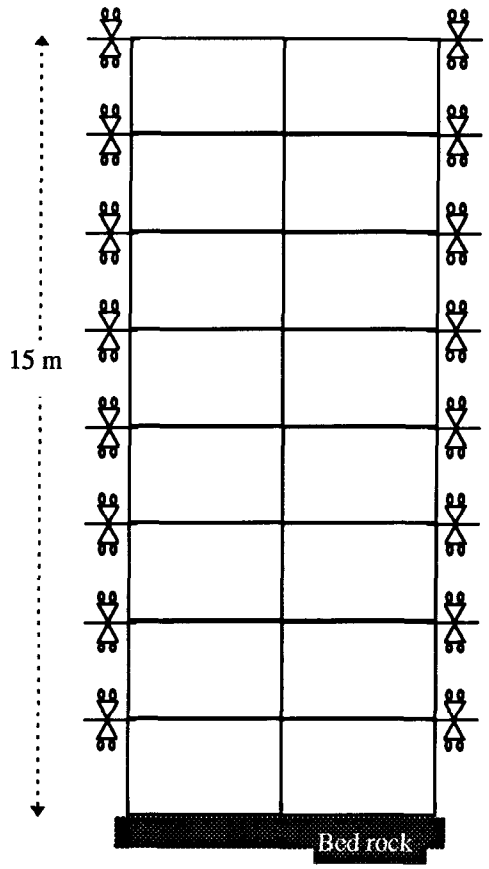

Fig.3 Schematic representation of the FE mesh

data points plotted per complete transducer record

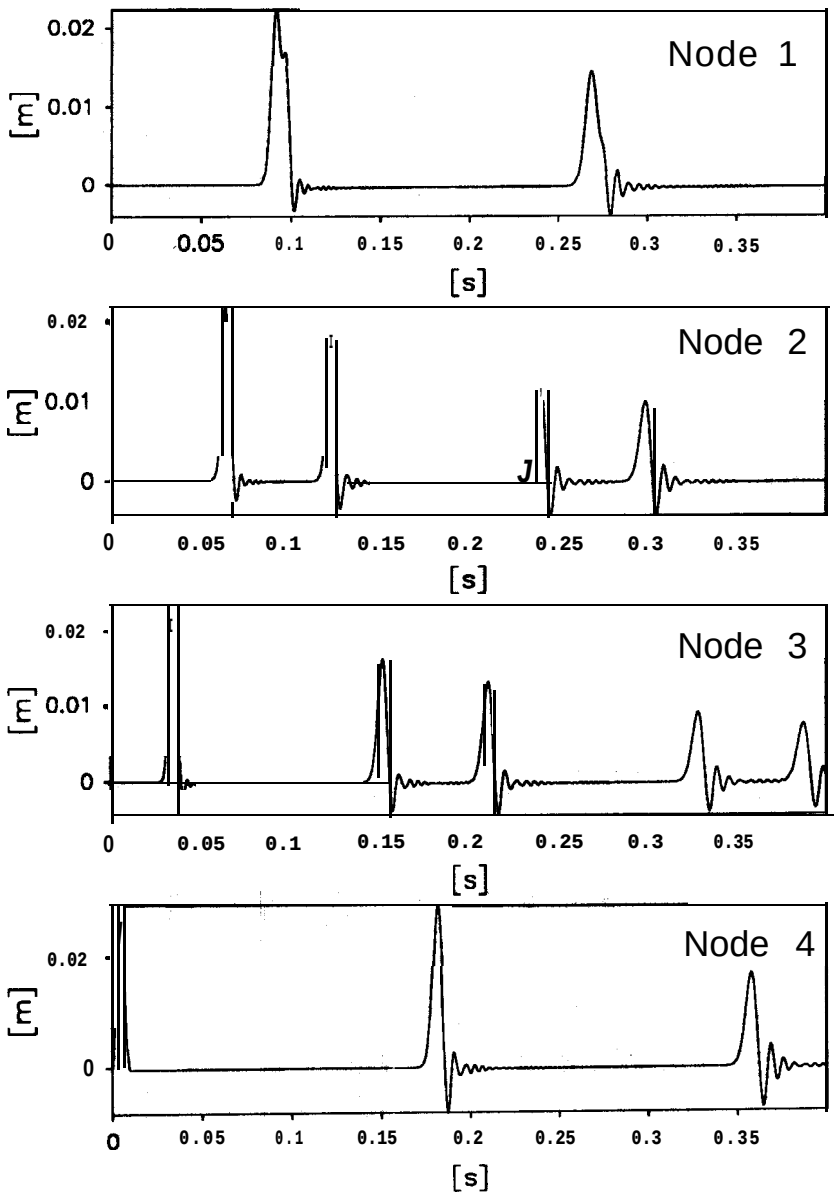

Scales : Model

TEST MODEL FLIGHT	vl	TIME RECORDS		FIG.NO. 4

data paints platted per complete transducer record

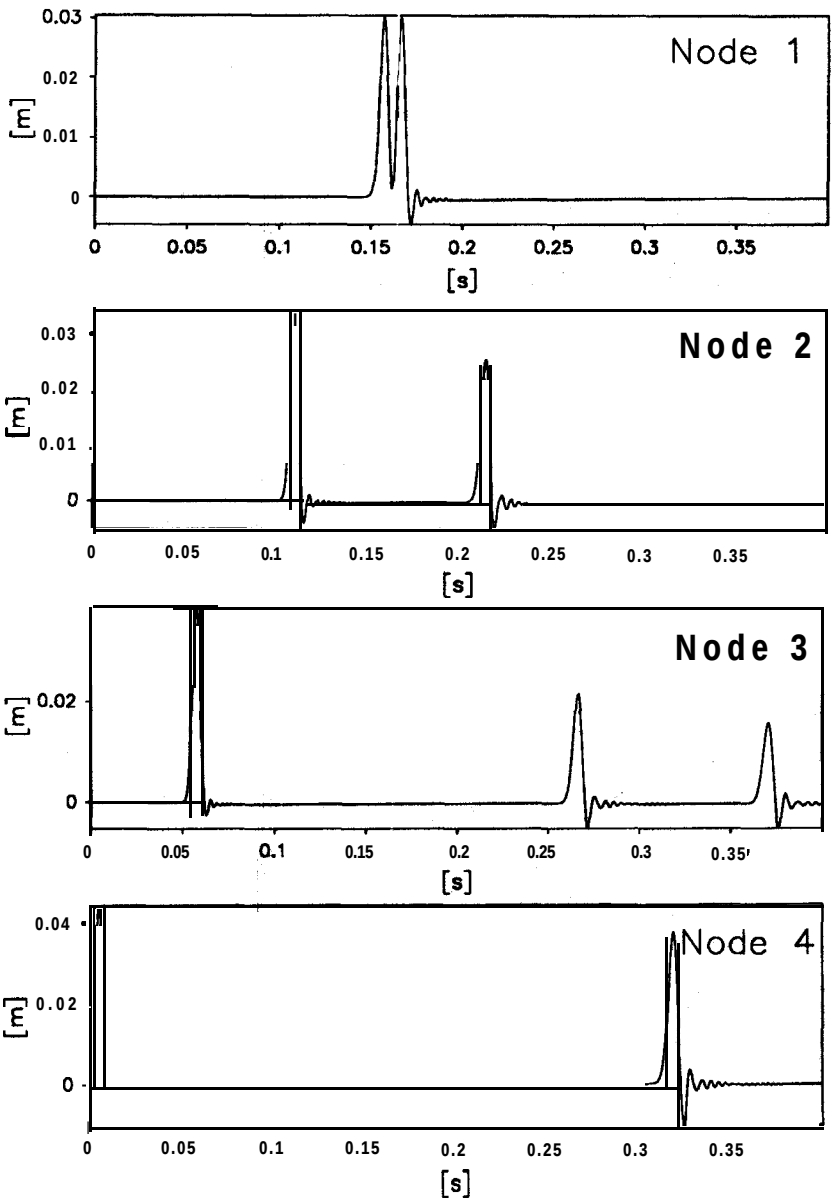

Scales : Model

TEST MODEL FLIGHT	v2	TIME RECORDS		FIG.NO. 5

data points plotted per complete transducer record

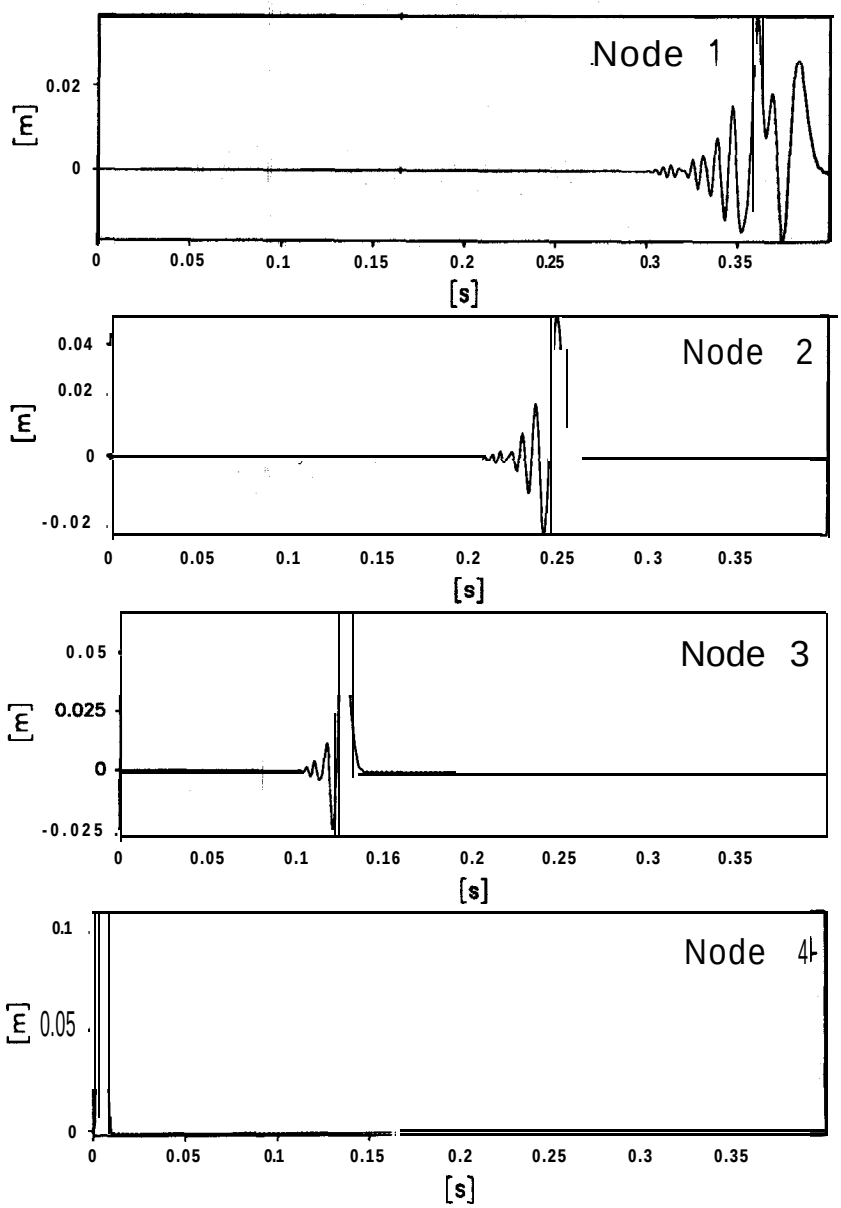

Scales : Model

TEST MODEL FLIGHT	v3 ,	TIME RECORDS		FIG.NO. 6

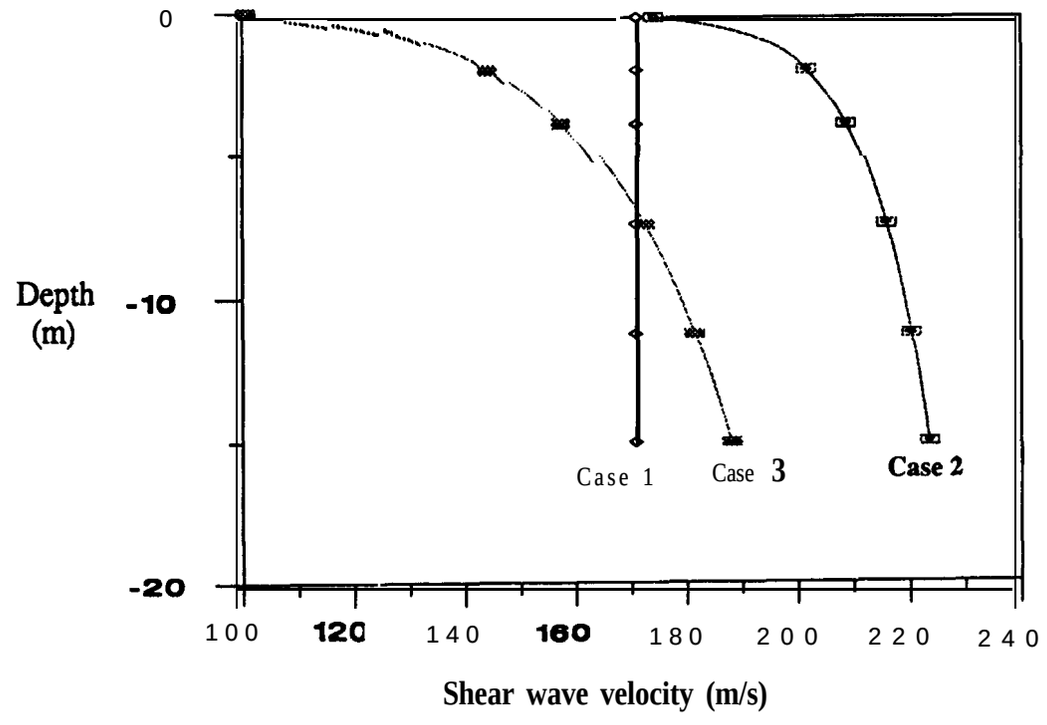

Fig.7 Variation of shear wave velocity with depth

data points plotted per complete transducer record

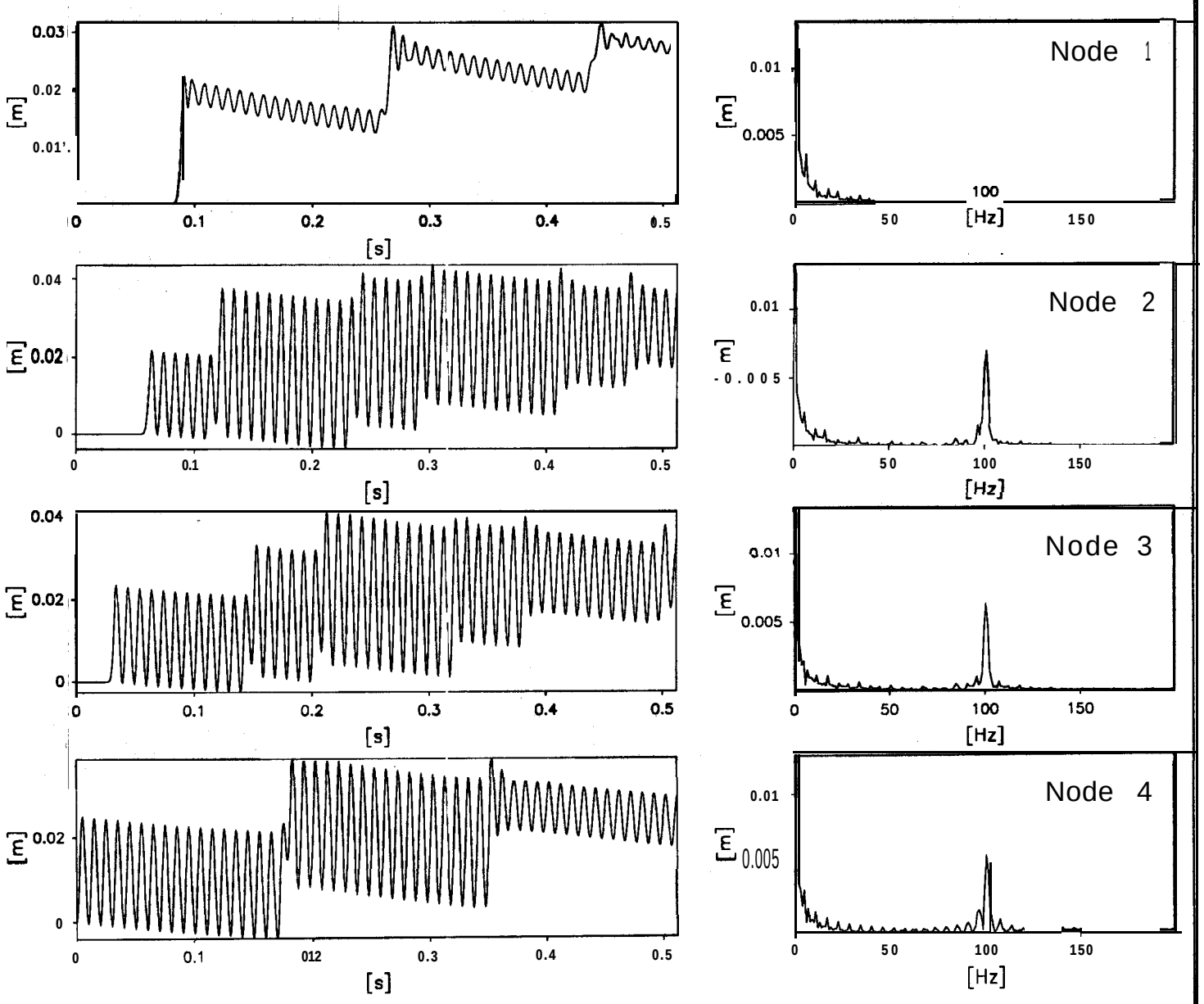

Scales : Model

TEST MODEL FLIGHT	ss1	TIME RECORDS		FIG.NO. 8

data points plotted per complete transducer record

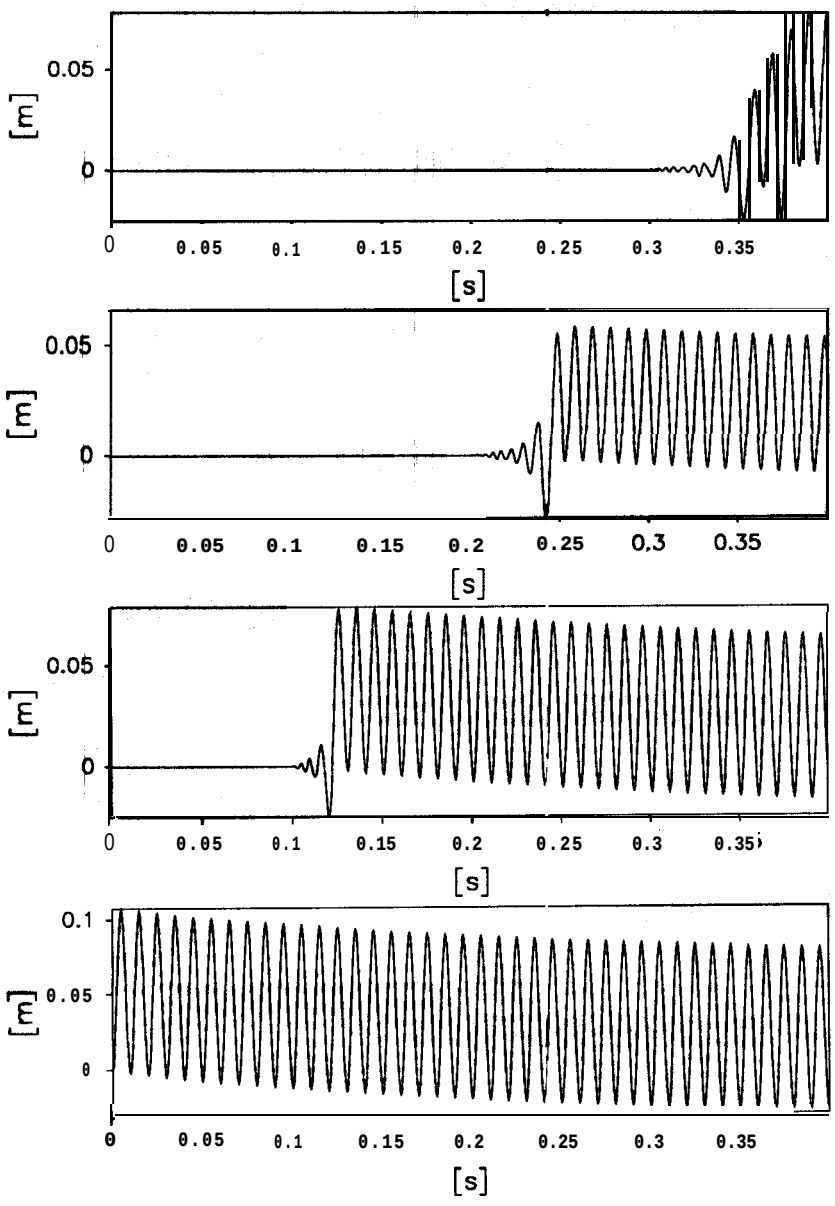

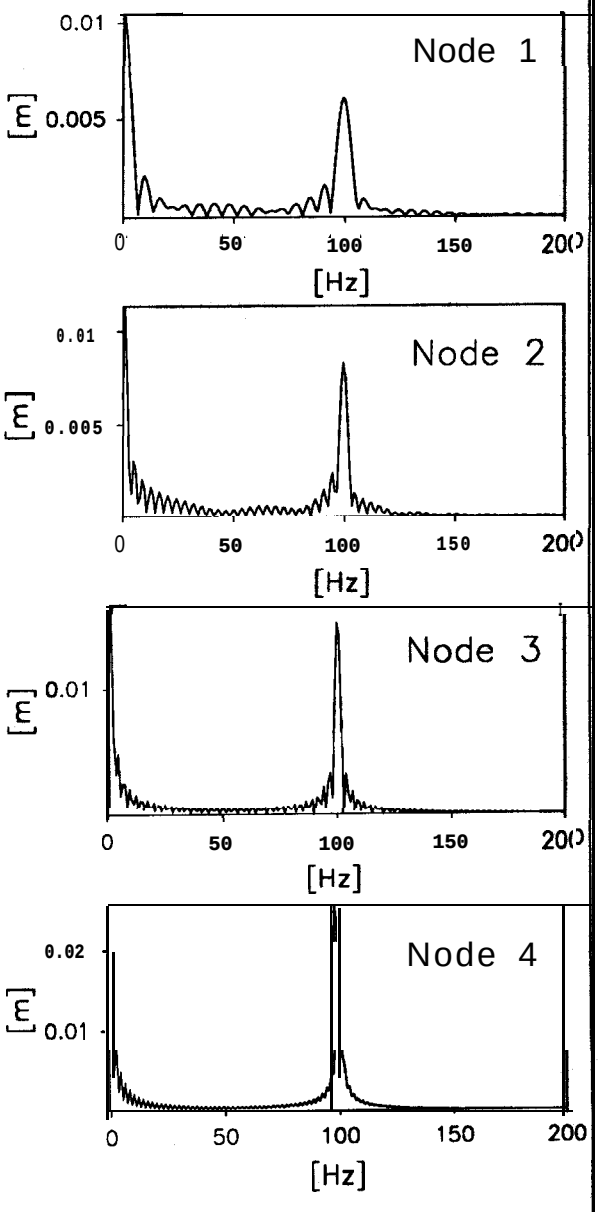

Scales : Model

TEST MODEL FLIGHT	ss2	TIME RECORDS		FIG.NO. 9

data points plotted per complete transducer record

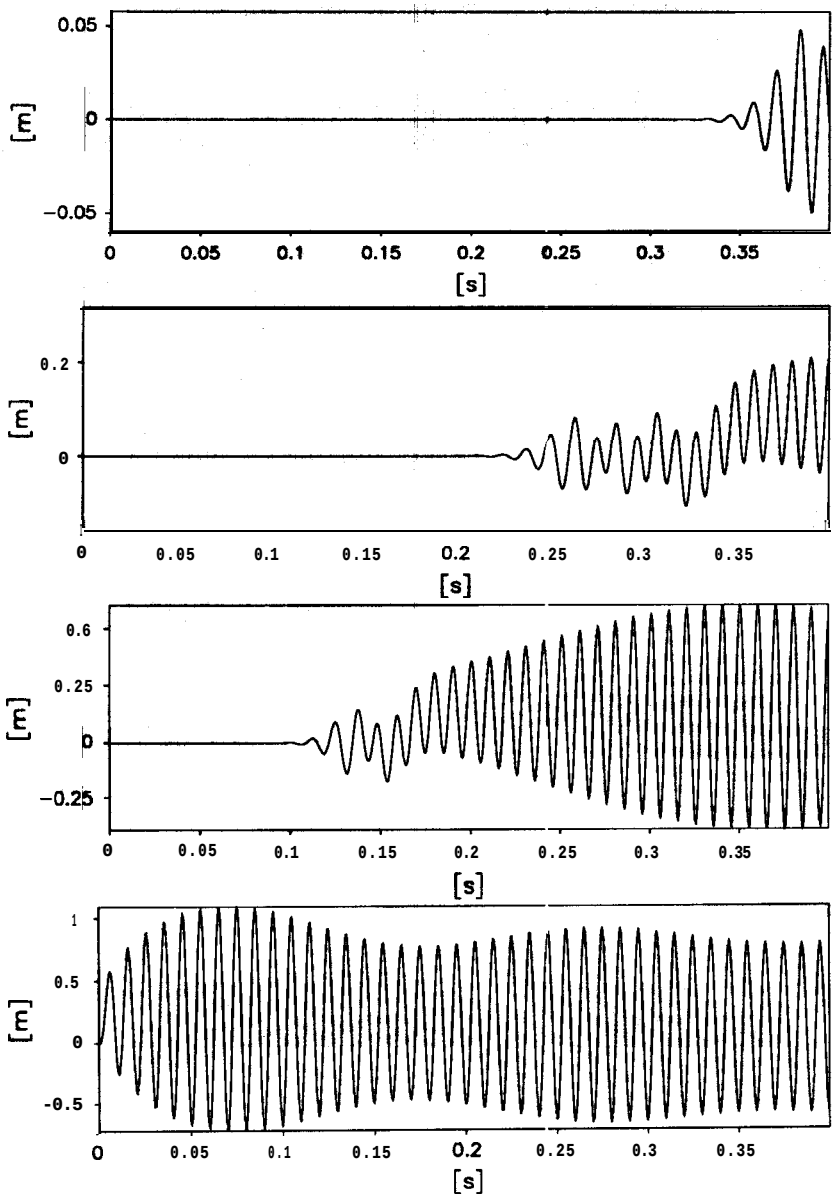

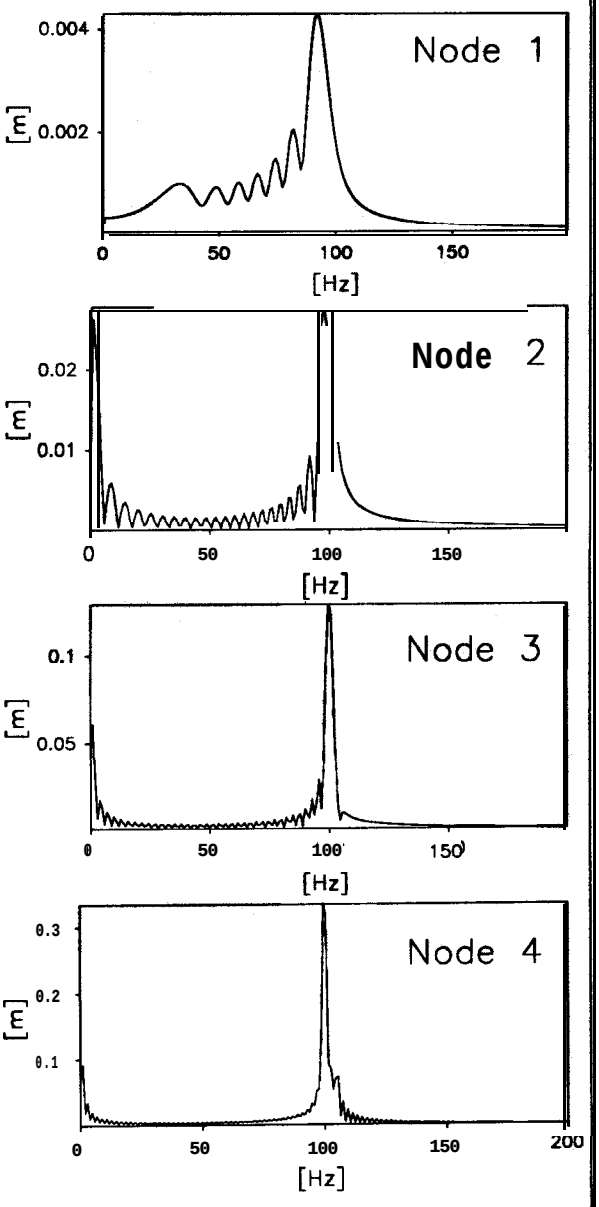

Scales : Model

TEST MODEL FLIGHT	**ss3**	**TIME RECORDS**		FIG.NO. **10**

data points plotted per complete transducer record

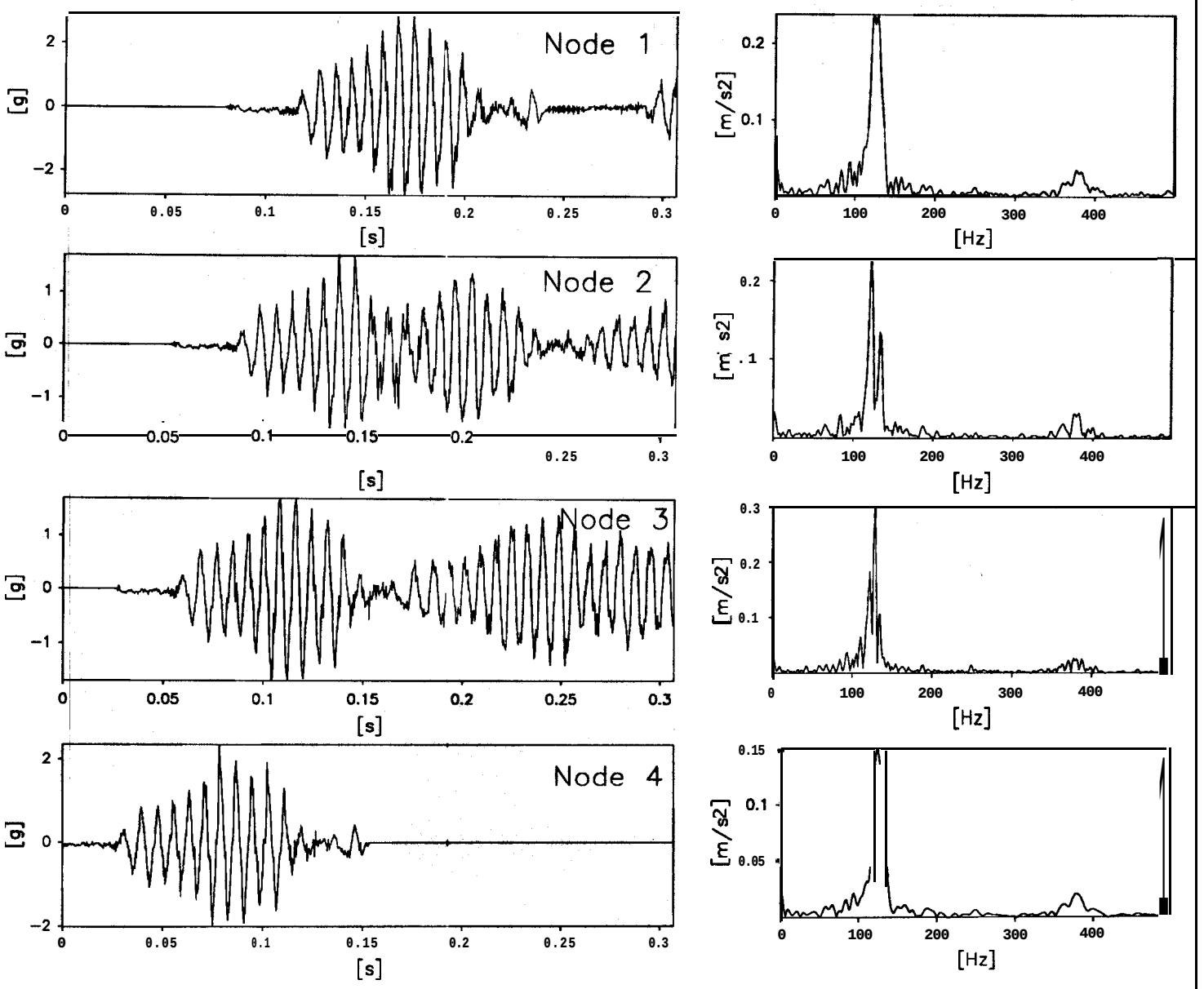

Scales : Model

TEST				
MODEL FLIGHT	BB1	TIME RECORDS		FIG.NO. 11

data points plotted per complete transducer record

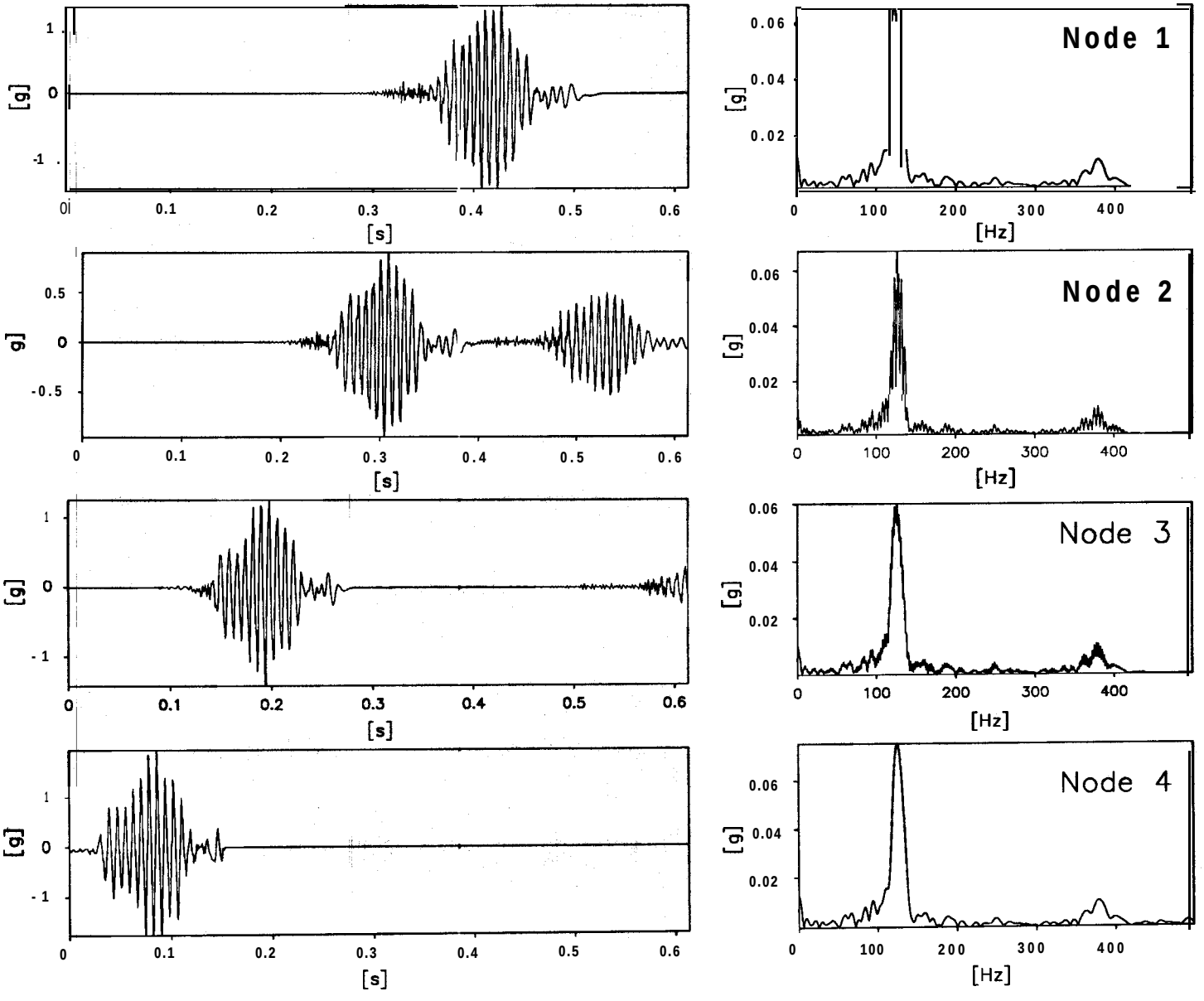

Scales : Model

TEST MODEL FLIGHT	bb2	TIME RECORDS		FIG.NO. 12

data points plotted per complete transducer record

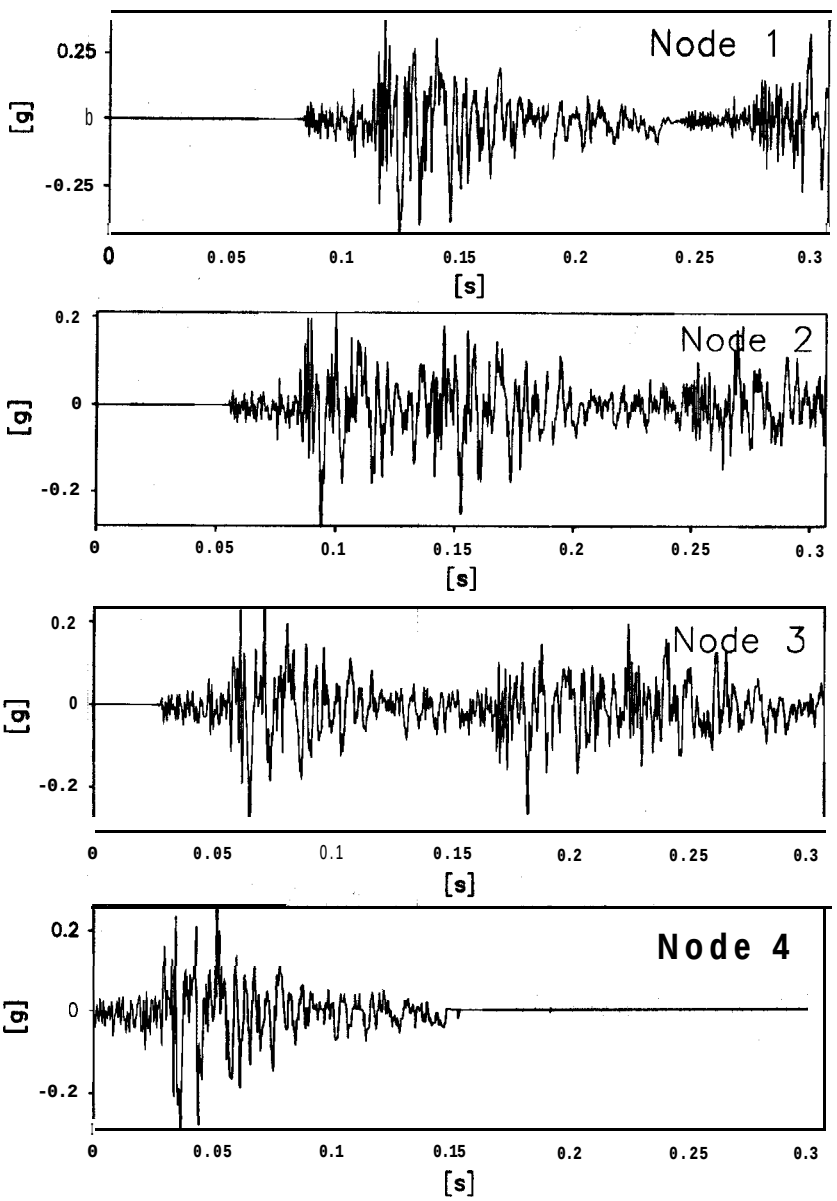

Scales : Model

TEST MODEL FLIGHT	LL1	TIME RECORDS		FIG.NO. 13

data points plotted per complete transducer record

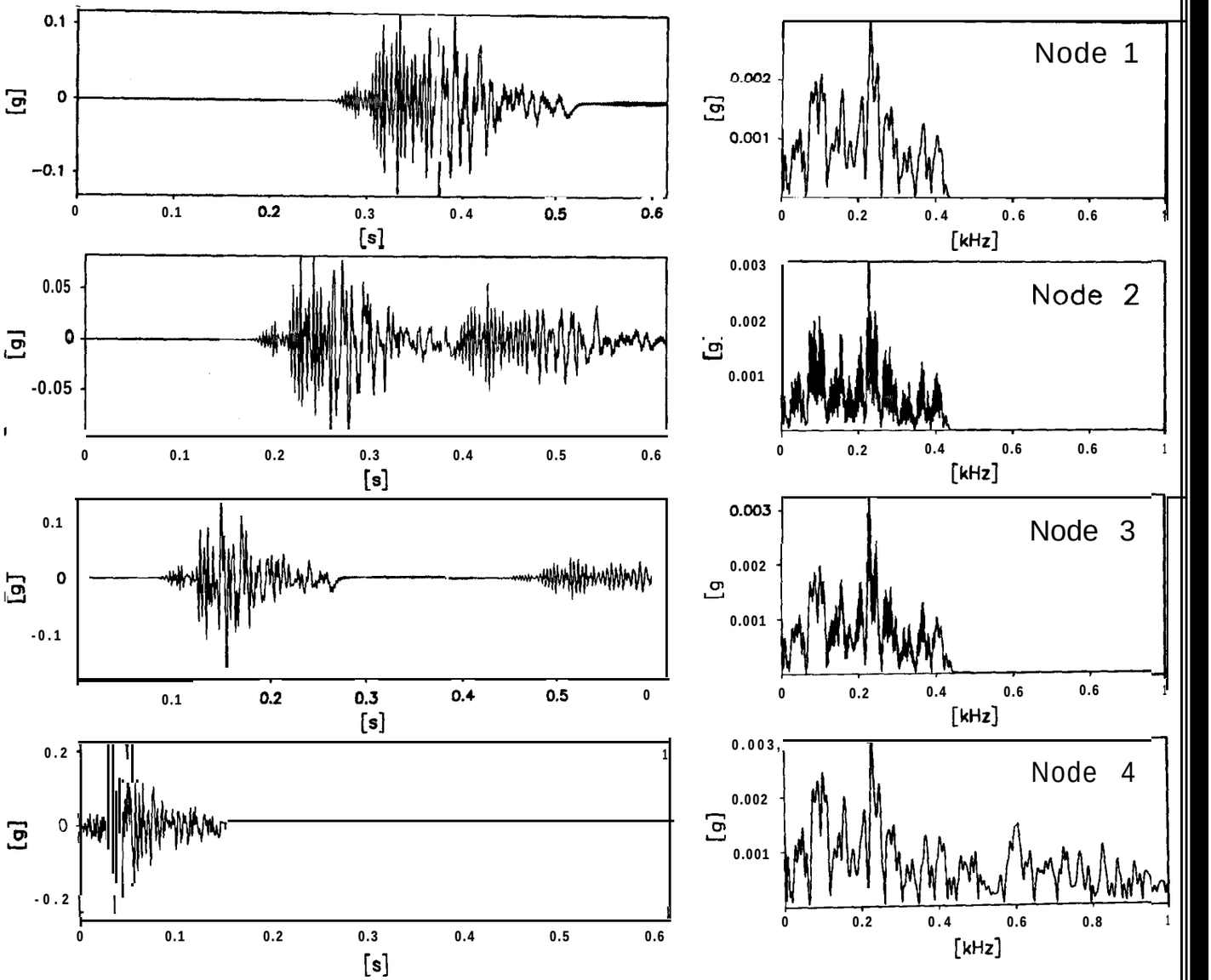

Scales : Model

TEST MODEL FLIGHT	LL2	TIME RECORDS		FIG.NO. 14